frontiers | Frontiers in Energy Research

TYPE Original Research
PUBLISHED 31 August 2023
DOI 10.3389/fenrg.2023.1258689

OPEN ACCESS

EDITED BY
Jianli Zhou,
Xinjiang University, China

REVIEWED BY
Linfei Yin,
Guangxi University, China
Xiong Wu,
Xi'an Jiaotong University, China

*CORRESPONDENCE
Youwen Tian,
youwen_tian10@163.com

RECEIVED 14 July 2023
ACCEPTED 14 August 2023
PUBLISHED 31 August 2023

CITATION
Zhang H, Tian Y, Zhao Y, Liu Q and Zhang N (2023), Economic dispatch of generation load aggregators based on two-stage robust optimization.
Front. Energy Res. 11:1258689.
doi: 10.3389/fenrg.2023.1258689

Economic dispatch of generation load aggregators based on two-stage robust optimization

Haonan Zhang[1], Youwen Tian[1]*, Yi Zhao[2], Qingyu Liu[1] and Nannan Zhang[1]

[1]School of Information and Power, Shenyang Agricultural University, Shenyang, Liaoning, China, [2]College of Electric Power, Shenyang Institute of Engineering, Shenyang, Liaoning, China

Introduction: In recent years, with the rapid development of renewable energy generation, the stability of the power grid has been greatly reduced. In response to this problem, integrating the user side transferable load into the power market has become the key to the development of future power grid. At present, large transferable loads have entered the electricity market in some pilot areas of China, but the relevant research on small and medium-sized transferable users entering the electricity market is still few.

Methods: This paper proposes the concept of generation load aggregators. A two-stage generation load aggregator robust optimization model is developed to obtain the scheduling scheme with the lowest operating cost under the worst scenario. The model consists of distributed renewable power, transferable load, self-provided power, energy storage, etc. Uncertainties of renewable energy and load are introduced in the model. By using the column constraint generation algorithm and strong pairwise theory, the original problem is decomposed into the main problem and sub-problems to be solved alternately, so as to obtain the scheduling scheme with the lowest operating cost in the worst scenario under different conservatism.

Results: The solved results are compared with those without the generation load aggregator, illustrating the role of the generation load aggregator in relieving peak and valley pressure on the grid from the load side, reducing the cost of electricity for loads, and promoting the consumption of renewable energy. The comparison with the deterministic optimization algorithm shows a significant decrease in the total cost and validates the performance of the selected solution algorithm. The boundary conditions for the use of energy storage by generation load aggregators for peak and valley reduction under the time-sharing tariff mechanism are also derived.

Discussion: This study can provide reference for the investors of generation load aggregators when planning whether to install energy storage or the scale of energy storage, and also help the power market management department to design a reasonable incentive mechanism.

KEYWORDS

generation load aggregator, two-stage robust optimization, uncertainty optimization, economic dispatch, column constraint generation algorithm

1 Introduction

In recent years, with the rapid development of wind power, photovoltaic, and other renewable energy generation, the intermittent volatility of renewable energy generation has posed an increasing challenge to the power grid, and the problem of curtailed wind and PV caused by the balance of supply and demand power has become increasingly prominent. In addition, the gradual increase in the peak-to-valley load difference and the continuous growth of peak loads have reduced the stability of the safe operation of the power market (Li and Wang, 2021; Wu et al., 2022b; Sambodo et al., 2022). In response to the aforementioned problems, incorporating customer-side transferable loads into the power system has become the key to future grid development. Transferable loads are loads that actively respond to price signals and incentives to change the behavior of the original electricity consumption pattern (Chen et al., 2021). At this stage, large transferable loads have entered the power market in some pilot areas in China and are dispatched by the grid company. Research related to the access of small- and medium-sized transferable users to the power market remains scarce. To solve this problem, the concept of generation load aggregators is proposed in this paper. Small- and medium-sized transferable users sign agency contracts with generation load aggregators, and users participate in the electricity market through generation load aggregators. The generation load aggregator is mainly a load aggregator, which also aggregates distributed energy, energy storage, electric vehicles, self-provided generator on the load side, *etc.* Load aggregators are able to consolidate dispersed adjustable potential to form the scalable user-adjustable capacity that the market needs and respond to the grid's price signals for profit (Li et al., 2022). When power consumption peaks or other periods of high electricity prices, power sources, and energy storage in generation load aggregators choose to operate at high power, at the same time, the transferable loads therein operate at as low a power as possible. When the power supply runs at a low power or even shuts down during low hours or other periods of lower electricity prices, the energy storage will charge and the transferable load will use electricity at a higher power at this time. The generation load aggregator participates in the market bidding for load regulation behavior as a demand response product, and the winning load resource is compensated with the corresponding market clearing price. The difference between generation load aggregators and electric power companies is that they do not make money in the same way. Electric power companies primarily make money by buying low and selling high. Generation load aggregators earn grid regulation fees primarily by regulating electricity use. The difference between generation load aggregators and microgrids is in the integrity of the system. Microgrids are smaller, decentralized, stand-alone systems that can be operated individually for extended periods. The generation load aggregators rely mainly on purchasing power in the electricity market, where the captive power supply is not sufficient to support the load for a long period. The difference between generation load aggregators and virtual power plants is their different roles in the electricity market. The virtual power plant belongs to the generation side, and the generation load aggregator is effectively an adjustable electricity consumer.

Economic scheduling of aggregators is a hot issue in research related to aggregators, generally intending to minimize operating costs. Smaller operating costs with constant revenues imply higher profits (Iria et al., 2020; Kim et al., 2022). Zhang et al. developed a two-stage optimization model for industrial load aggregators considering the uncertainty of load response and the satisfaction of users (Zhang et al., 2018). Xu et al. established an optimal scheduling model for an electric vehicle charging aggregator to solve the profit maximization of the aggregator by genetic algorithm (Xu et al., 2020). With the development of distributed energy sources, energy storage, *etc.*, aggregators contain not only industrial and residential loads but also distributed power output from photovoltaic, wind power, *etc.*, and the stochastic nature of load power consumption brings challenges to the operation of aggregators (Sheikhahmadi et al., 2018). How to effectively cope with the uncertainties within the aggregator and achieve reliable and economical operation has become the key to the study of the economic scheduling problem of aggregators (Xu et al., 2020). For such problems, stochastic programming is often used to model uncertain variables and simulate the impact of uncertainty on the operation of aggregators' stochastic programming which uses random variables to describe uncertain information and optimizes to obtain the scheduling solution with the minimum expected cost (Kim et al., 2021). The key to stochastic programming is to model uncertain variable properties with a limited number of scenarios (Wang and Nie, 2022). Vahid-Ghavidel proposed a hybrid stochastic optimization model to deal with electricity market price and consumer participation rate uncertainty (Vahid-Ghavidel et al., 2021). Vatandoust described the joint optimization of electric vehicles and energy storage aggregators in the day-ahead electricity market to improve the profitability of the aggregators with a stochastic mixed integer linear programming model considering the uncertainty of energy and frequency regulation prices (Vatandoust et al., 2019). Since stochastic programming methods seek the solution set with the maximum/minimum expected value of the objective function, the risk of irrational decision making exists for a certain scenario. Nguyen combined stochastic programming and conditional value-at-risk constraint methods so that the expected return in the corresponding scenario is not lower than the given confidence level, thus reducing the system risk (Nguyen and Le, 2015). However, both stochastic programming and scenario analysis methods require deterministic probability curves to generate scenarios, which may lead to models that are not accurate enough to reflect the actual situation (Wang et al., 2015a).

Compared with the aforementioned methods, robust optimization replaces the exact probability distribution of random variables with an uncertainty set and obtains the scheduling solution of the system under the "worst-case" scenario through optimization, which is more suitable for practical engineering needs (Alvim et al., 2021). Lu considered the uncertainty of charging and discharging of EV aggregators, built a two-stage robust optimization model, used distributed robust optimization to improve the average economic performance of the model, and applied Farkas' Lemma and robust optimization to ensure the safety of the distribution system operation (Lu et al., 2021). Najafi proposed a hybrid decentralized robust optimization-

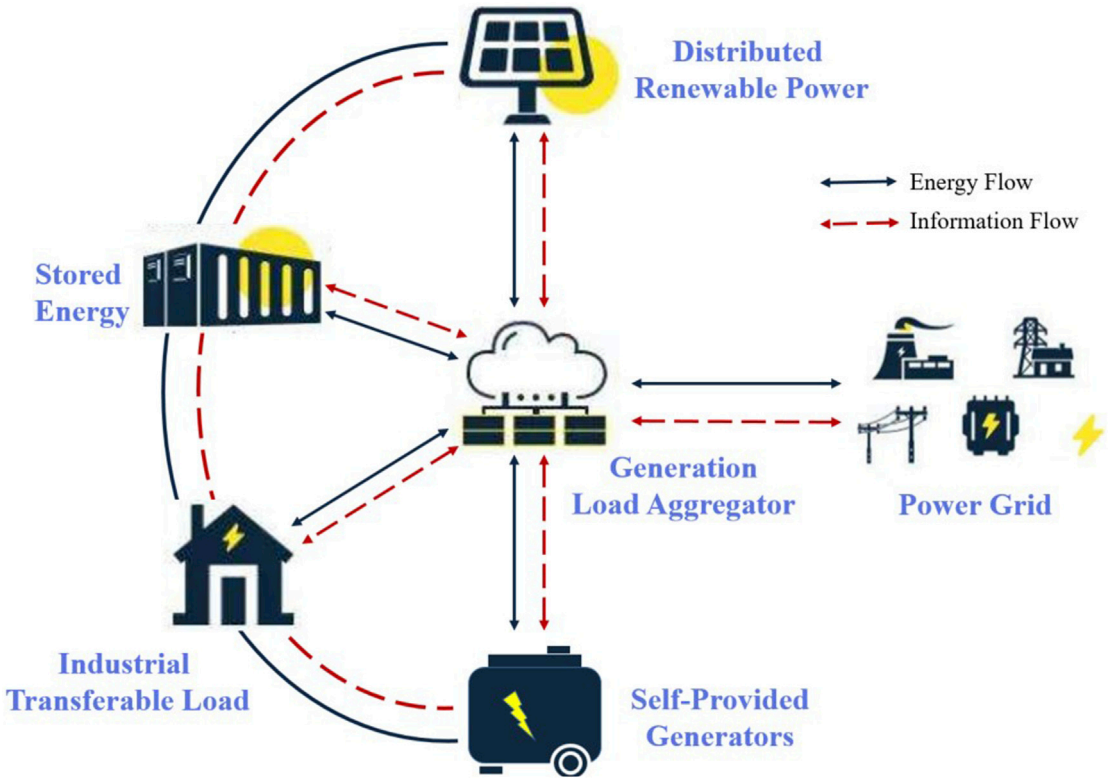

FIGURE 1
Structure of generation load aggregators.

stochastic programming (DRO-SP) model based on the multiplicative alternating direction method to coordinate the optimization of load aggregators, using a stochastic programming approach to model the uncertainty of the electric vehicle model and a robust optimization approach to model the uncertainty of the location marginal price (Najafi et al., 2021). Wang proposed a distribution uncertainty model where the probability distribution of load power can vary around a given reference distribution (Wang et al., 2015b). However, the robust models in the aforementioned literature do not allow for flexible adjustment of the conservativeness of the scheduling scheme.

The main contributions of this research can be summarized as follows.

1. To solve the problem that small- and medium-sized adjustable users on the load side are difficult to enter the electricity market, this paper proposes the concept of generation load aggregators for the first time. The basic framework of the generation load aggregator is built, and a robust optimization model of a two-stage generation load aggregator with a min–max–min structure is established.
2. The model considers the coordinated control of PV power sources, load uncertainty, energy storage, two types of industrial transferable loads, and distributed power sources within the generating load aggregator. Using a column-constrained generation algorithm and strong pairwise theory obtains an economic dispatch scheme for the worst-case scenario under different conservatisms. Uncertainty adjustment parameters have been added to the scheme to provide flexibility in choosing the degree of conservatism in the scheduling scheme.
3. The solved results are compared with other sets of results to determine that the generation load aggregator model has the effect of relieving the peak and valley pressure on the grid, reducing the cost of electricity for loads, and promoting the consumption of renewable energy. The dispatch program obtained can withstand the risk of real-time market price fluctuations in electricity. We derive the boundary conditions for the analytical model to use energy storage for peak shaving and valley filling under the time-of-day tariff mechanism, which will provide a theoretical basis for the future construction planning of generation load aggregators as well as the entry of small- and medium-sized adjustable users into the electricity market.

The main study of this paper is as follows. The first part, as the introductory part of the article, briefly introduces the background of the study as well as the research progress on the issues related to generation load aggregators in recent years. The second part builds the framework of the generation load aggregator system. The third part is to develop a two-stage robust optimization model for generation load aggregators. The fourth part is the numerical simulation and the related discussion and analysis of the results. The fifth part is the summary of the paper and the prospect of future research.

2 Materials and methods

2.1 Generation load aggregator system framework

Figure 1 shows the basic framework of a generation load aggregator, which consists of a collection of distributed PV, self-provided generator, energy storage, transferable load, and other components. The transferable load can be divided into the start/stop time delay-type transferable load and power sizing-type transferable load due to the actual needs of the industry. Generation load aggregators provide an opportunity for small- and medium-sized customers to participate in the regulation of the electricity market. Small- and medium-sized customers do not reach the minimum level of load elasticity to participate in demand response and cannot find a way to participate in power trading. As an intermediary, a generation load aggregator can integrate customer demand response resources and bring them into the market for trading, making idle load resources useful while relieving the pressure on the power system from the load side during special times such as peak and valley. On the other hand, power generation load aggregators fully explore the potential of load demand response, under the help and guidance of power generation load aggregators, and form a scientific and economic way of electricity consumption, to reduce the cost of electricity for users. The generation load aggregator needs to summarize the electricity consumption curve of the load on D-1, the generation curve of each power source, and the curve of the need to buy or sell electricity from the external grid before day D. If the reported curve is different from the actual curve, it needs to buy or sell electricity from the external grid.

2.1.1 Self-provided generator

The self-provided generator of the generation load aggregators are mainly micro-gas turbines, and the cost of micro-gas turbine generation C_G^t can be expressed as a linear function (Wang et al., 2015b).

$$C_G^t = [aP_G^t + b]\Delta t, \tag{1}$$

where a and b are cost coefficients; P_G^t is the output power of the micro-gas turbine in time slot t; and Δt is the scheduling step, which takes the value of 1 h. The power response time of the micro-gas turbine is negligible compared to the hourly scheduling step, so the ramping constraint of the micro-gas turbine is not considered and only the output power constraint is considered.

$$P_G^{\min} \le P_G^t \le P_G^{\max}, \tag{2}$$

where $P_G^{\max}$ and $P_G^{\min}$ denote the maximum/minimum output power of the micro-gas turbine, and the maximum/minimum output power is limited by its rated power and minimum load factor, respectively.

2.1.2 Energy storage

The cost of energy storage C_S^t is mainly composed of the investment cost, operation cost, and maintenance cost of energy storage (Xu et al., 2010), and the average charging and discharging cost at time t during the payback period can be expressed as

$$C_S^t = K_S\left[\frac{P_S^{t,dis}}{\eta} + P_S^{t,ch}\eta\right]\Delta t, \tag{3}$$

where K_S is the unit charge/discharge cost of energy storage after considering investment cost, operation cost, and maintenance cost; $P_S^{t,ch}$ and $P_S^{t,dis}$ denote the charge/discharge power of energy storage in time t; and η is the charge/discharge efficiency of energy storage, respectively. The constraints to be satisfied during the operation of energy storage include

$$0 \le P_S^{t,dis} \le \alpha_S^t P_S^{\max}, \tag{4}$$

$$0 \le P_S^{t,ch} \le [1 - \alpha_S^t]P_S^{\max}, \tag{5}$$

$$\eta\sum_{t=1}^{N}\left[P_S^{t,ch}\Delta t\right] - \frac{1}{\eta}\sum_{t=1}^{N}\left[P_S^{t,dis}\Delta t\right] = 0, \tag{6}$$

$$E_S^{\min} \le E_S^0 + \eta\sum_{t=1}^{N}\left[P_S^{t,ch}\Delta t\right] - \frac{1}{\eta}\sum_{t=1}^{N}\left[P_S^{t,dis}\Delta t\right] \le E_S^{\max}. \tag{7}$$

Equation 4 and Equation 5 are the charging/discharging power constraints of energy storage, which are the maximum charging/discharging power of energy storage, mainly limited by the capacity of the grid-connected inverter, respectively. α_S^t indicates the charging/discharging state of energy storage, $\alpha_S^t = 1$ indicates that energy storage is discharged in time t and $\alpha_S^t = 0$ indicates that energy storage is charged in time t. Equation 6 is the constraint to ensure that the power stored in energy storage at the beginning and end of the dispatch cycle is equal, which is conducive to the cyclic scheduling of energy storage, and N is the scheduling cycle and takes the value of 24. Equation 7 indicates the power constraint of energy storage in each time, E_S^0 is the power of energy storage at the initial moment of scheduling, and $E_S^{\max}$ and $E_S^{\min}$ are the maximum/minimum power allowed for energy storage during the scheduling process, respectively, and the main purpose of this constraint is to prevent energy storage from overcharging or over discharging to prolong its service life.

2.1.3 Transferable load

Industrial loads have some differences in control and scheduling methods due to different factors such as industry, production shift system, and operation of power-using equipment. Most industrial transferable loads can be divided into two categories: start–stop time delay and power size regulation (Kumar et al., 2022).

2.1.4 Start–stop time delay transferable load

The start–stop time delay of transferable load is a more common type of transferable load. Except for the start–stop periods, the start–stop time delay class of transferable loads consumes relatively flat power for most of the work cycle. And with thermal inertia, starting after a short delay does not affect production. However, the load curve must shift in time as a whole, as shown in Figure 2A.

The power consumed by the start–stop time delay type of transferable loads is shown as follows:

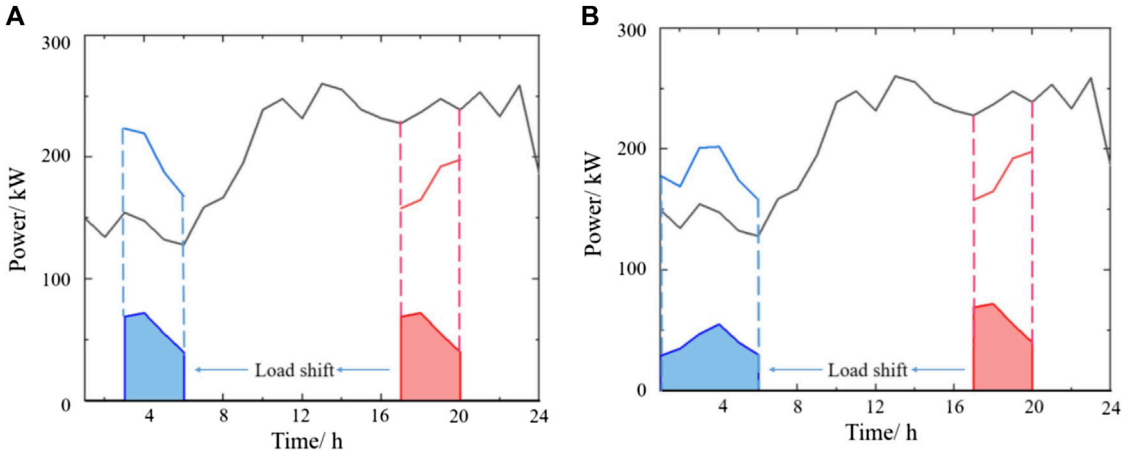

FIGURE 2
(A) Schematic diagram of start–stop time delay transferable load and **(B)** schematic diagram of power sizing transferable load.

$$P_{QT}^{t} = \begin{cases} 0 & t \le t_{on} \\ \dfrac{P_e^t}{\Delta t_{up}}(t - t_{on}) & t_{on} \le t \le t_{on} + \Delta t_{up} \\ (1 + \delta(t))P_e^t & t_{on} + \Delta t_{up} \le t \le t_{off} - \Delta t_{down}, \\ \dfrac{P_e^t}{\Delta t_{down}}\left(t_{off} - t\right) & t_{off} - \Delta t_{down} \le t \le t_{off} \\ 0 & t \ge t_{off} \end{cases} \quad (8)$$

where P_{QT}^{t} is the actual dispatch power of the generation load aggregator for the transferable load at time t; t_{on} is the power-on time of transferable load; and Δt_{up} is the time it takes from power-on to stability. Δt_{down} is the time required to shut down the equipment until the power is 0; t_{off} is the moment when the power is 0; P_e^t is the rated power of transferable load; and $\delta(t)$ is the fluctuating power coefficient when the transferable load reaches the steady-state operation, usually 5%–20%.

Considering the case where the generation load aggregator contains a start–stop time delay type of transferable load, its electricity consumption characteristics in providing load regulation services can be expressed by the following constraint:

$$\sum_{t=1}^{N} P_{QT}^{t} \Delta t = D_{QT}, \quad (9)$$

$$D_{QT}^{t,\min} \le P_{QT}^{t} \Delta t \le D_{QT}^{t,\max}, \quad (10)$$

where D_{QT} is the total electricity demand of the transferable load during the dispatch cycle and $D_{QT}^{t,\max}$ and $D_{QT}^{t,\min}$ are the maximum/minimum electricity demand of the transferable load at time t, related to the customer's requirements for its efficiency, respectively.

Since the daily load of the start–stop time delay transferable load is relatively stable, the starting and interruption time of each start–stop time delay transferable load is relatively fixed. The power plan of the transferable load can be adjusted, and the regulation of the transferable industrial load can be achieved by appropriately advancing or delaying the start/stop time. However, the change in the schedule will affect the industrial customers' habitual use of electricity. Therefore, the generation load aggregator needs to be compensated appropriately, and the dispatch cost C_{QT}^{t} can be expressed as

$$C_{QT}^{t} = K_{QT}\left|P_{QT}^{t} - P'^{,t}_{QT}\right|\Delta t, \quad (11)$$

where K_{QT} is the unit dispatch cost of the start–stop time delay transferable load and $P'^{,t}_{QT}$ is the expected power of the start–stop time delay transferable load at time t. The absolute value term in Eq. 11 represents the deviation between the actual power and the desired power, which can be reduced to the linear form shown in Eq. 12 by introducing auxiliary variables P_{QT1}^{t} and P_{QT2}^{t} and constraints (13–14).

$$C_{QT}^{t} = K_{QT}\left[P_{QT1}^{t} + P_{QT2}^{t}\right]\Delta t, \quad (12)$$

$$P_{QT1}^{t} - P'^{,t}_{QT1} + P_{QT2}^{t} - P'^{,t}_{QT2} = 0, \quad (13)$$

$$P_{QT1}^{t} \ge 0, P_{QT2}^{t} \ge 0. \quad (14)$$

2.1.5 Power sizing transferable load

Power sizing transferable load is another common type of regulated industrial load. This type of load reduces the peak-to-valley load difference and reduces operating costs by transferring the power size during peak hours to other load hours, as shown in Figure 2B.

The power of the transferable load of the power sizing type can be expressed by the following equation:

$$P_{TJ}^{t} = P_e^{'} + \alpha_t P_{e,\max}^{'} \quad (15)$$

where P_{TJ}^{t} is the actual power dispatched by the generation load aggregator to the transferable load in time t and $P_e^{'}$ is the average power consumption of power size regulation transferable load. $P_{e\ \max}^{'}$ is the maximum regulation power. α_t is the participation adjustment factor, when $\alpha_t > 0$, power increases and when $\alpha_t < 0$, power reduces. To ensure that the efficiency of work does not change, the power size adjustment type can transfer the load to increase and reduce the total amount of power used equally.

Considering the case of a generation load aggregator that contains a transferable load of the power sizing regulation type, its electricity consumption characteristics during the provision of

load regulation services can be expressed by the following constraint:

$$\sum_{t=1}^{N} P_{TJ}^{t} \Delta t = D_{TJ}, \tag{16}$$

$$D_{TJ}^{t,\min} \le P_{TJ}^{t} \Delta t \le D_{TJ}^{t,\max}, \tag{17}$$

where D_{TJ} is the total demand of the transferable load in a dispatch cycle and $D_{TJ}^{t,\max}$ and $D_{TJ}^{t,\min}$ are the maximum/minimum demand of the transferable load in time t, respectively.

The power sizing transferable load can also flexibly adjust the demand response load schedule, but the generation load aggregator also needs to compensate the transferable load enterprise, and the dispatch cost C_{TJ}^{t} required for time t can be expressed as

$$C_{TJ}^{t} = K_{TJ} \left| P_{TJ}^{t} - P'^{t}_{TJ} \right| \Delta t, \tag{18}$$

where K_{TJ} is the unit dispatch cost of the power sizing load and P'^{t}_{TJ} is the expected power consumption of the power sizing load at time t. The absolute value term in Eq. 18 is used to represent the deviation between the actual dispatched power and the desired power consumption, which can be reduced to the linear form shown in Eq. 19 by introducing auxiliary variables P_{TJ1}^{t} and P_{TJ2}^{t} and constraints (20–21).

$$C_{TJ}^{t} = K_{TJ} \left[P_{TJ1}^{t} + P_{TJ2}^{t} \right] \Delta t, \tag{19}$$

$$P_{TJ1}^{t} - P'^{t}_{TJ1} + P_{TJ2}^{t} - P'^{t}_{TJ2} = 0, \tag{20}$$

$$P_{TJ1}^{t} \ge 0, P_{TJ2}^{t} \ge 0. \tag{21}$$

2.1.6 External grid-interactive power

When the self-provided generator, renewable energy, and energy storage within the generation load aggregator cannot meet the load demand, it needs to purchase power from the external grid; conversely, the generation load aggregator can sell the surplus power to the external grid to obtain revenue (Jiang et al., 2021). The interactive power between the generation load aggregator and the external grid is subject to the following balancing constraints:

$$P_{M}^{t,buy} - P_{M}^{t,sell} = P_{S}^{t,ch} + P_{QT}^{t} + P_{TJ}^{t} + P_{L}^{t} - P_{G}^{t} - P_{S}^{t,dis} - P_{PV}^{t}, \tag{22}$$

where $P_{M}^{t,buy}$ and $P_{M}^{t,sell}$ are the power of the generation load aggregator to buy or sell electricity to the external grid in time t, respectively. Wind power is rarely located in industrial areas due to large land areas and other factors. Therefore, in this paper, only renewable power sources are considered for photovoltaic power generation. P_{PV}^{t} is the PV output power of the generation load aggregator in time t. P_{L}^{t} is the conventional load power in time t.

The interactive power between the generation load aggregator and the external grid needs to satisfy

$$0 \le P_{M}^{t,buy} \le \alpha_{M}^{t} P_{M}^{\max}, \tag{23}$$

$$0 \le P_{M}^{t,sell} \le \left[1 - \alpha_{M}^{t} \right] P_{M}^{\max}, \tag{24}$$

where $P_{M}^{\max}$ is the maximum value of the power exchanged between the load aggregator and the external grid, which is determined by considering the capacity of the transformer at the connection between the external grid and the load aggregator and the specific policies. α_{M}^{t} is the purchase and sale status of the load aggregator to the external grid, $\alpha_{M}^{t} = 1$ is the purchase of power by the load aggregator to the external grid, and $\alpha_{M}^{t} = 0$ is the sale of power by the load aggregator to the external grid. In time t, interaction cost C_{M}^{t} between the load aggregator and the external grid can be expressed as

$$C_{M}^{t} = \lambda_{t} \left[P_{M}^{t,sell} - P_{M}^{t,buy} \right] \Delta t, \tag{25}$$

where λ_{t} is the day-ahead traded tariff of the external grid.

2.2 Two-stage robust optimization model

The generation load aggregator model has the minimum daily operating cost as the optimization objective, as shown in Eq. 22, and the model constraints include Eq. 2, Eq. 4–Eq. 7, Eq. 9–Eq. 14, Eq. 16–Eq. 21, and Eq. 23–Eq. 24.

$$\min C = \sum_{t=1}^{N} \left[C_{G}^{t} + C_{S}^{t} + C_{QT}^{t} + C_{GL}^{t} + C_{M}^{t} \right]. \tag{26}$$

When the uncertainties of PV and load are not considered, the deterministic optimization model for the aforementioned generation load aggregator economic dispatch problem can be formulated in a compact form as

$$\begin{cases} \min\limits_{x,y} \boldsymbol{c}^{T} \boldsymbol{y} \\ s.t. \boldsymbol{A}\boldsymbol{y} \ge \boldsymbol{d} \\ \boldsymbol{K}\boldsymbol{y} = \boldsymbol{0} \\ \boldsymbol{G}\boldsymbol{x} + \boldsymbol{E}\boldsymbol{y} \ge \boldsymbol{h} \\ \boldsymbol{I}_{u}\boldsymbol{y} = \widehat{\boldsymbol{u}}, \end{cases} \tag{27}$$

where $\boldsymbol{x}$ and $\boldsymbol{y}$ are optimization variables, and the specific expressions are

$$\begin{cases} \boldsymbol{x} = \left[U_{S}^{t}, U_{M}^{t} \right]^{T} \\ \boldsymbol{y} = \left[P_{G}^{t}, P_{S}^{t,ch}, P_{S}^{t,dis}, P_{QT}^{t}, P_{TJ}^{t}, P_{M}^{t,buy}, P_{M}^{t,sell}, P_{PV}^{t}, P_{L}^{t} \right]^{T}, t = (1, 2 \cdots N), \end{cases} \tag{28}$$

where c is the objective function (26) column vector coefficients; $\boldsymbol{A}$, $\boldsymbol{K}$, $\boldsymbol{G}$, $\boldsymbol{E}$, and $\boldsymbol{I}_{u}$ are the coefficient matrices of the variables under the corresponding constraints; and $\boldsymbol{d}$ and $\boldsymbol{h}$ are constant column vectors. In Eq. 27, the first row of the constraints represents the inequality constraints in the generation load aggregator model, including Eq. 2, 7, Eq. 10, Eq. 14, Eq. 17, and Eq. 21. The second row is the equality constraint, including Eqs. 6 and 9, Eq. 12, Eq. 13, Eq. 17, Eq. 19, and Eq. 20. The third row corresponds to Eq. 4 and Eq. 5 and Eq. 23 and Eq. 24. Line 4 indicates that in the deterministic optimization model, the PV and load take the corresponding predicted values in time t, where

$$\widehat{\boldsymbol{u}} = \left[\widehat{u}_{PV}^{t}, \widehat{u}_{L}^{t} \right]^{T} t = (1, 2 \cdots N), \tag{29}$$

where $\widehat{u}_{PV}^{t}$ and $\widehat{u}_{L}^{t}$ denote the predicted values of PV output and load power in time t, respectively.

The aforementioned model is a mixed-integer linear programming problem, which can be solved by deterministic optimization methods, and the optimal solution depends on the accuracy of the predicted values. However, generation load aggregators are affected by many stochastic factors, which makes it difficult to guarantee prediction accuracy. In summary, deterministic optimization schemes often appear to be too “risky."

Therefore, in practice, the impact of uncertainty on the model needs to be accounted for. The box uncertainty set $\boldsymbol{U}$ considers the fluctuation range of PV output and load power.

$$\boldsymbol{U}=\begin{cases} u=\left[u_{PV}^{t},u_{L}^{t}\right]^{T}\in\mathbb{R}^{(N)\times 2},t=1,2\cdots N \\ u_{PV}^{t}\in\left[\widehat{u}_{PV}^{t}-\Delta u_{PV}^{t,\max},\widehat{u}_{PV}^{t}+\Delta u_{PV}^{t,\max}\right] \\ u_{L}^{t}\in\left[\widehat{u}_{L}^{t}-\Delta u_{L}^{t,\max},\widehat{u}_{L}^{t}+\Delta u_{L}^{t,\max}\right], \end{cases} \tag{30}$$

where u_{PV}^{t} and u_{L}^{t} are uncertain variables introduced into PV as well as load after adding uncertainty and $\Delta u_{PV}^{t,\max}$ and $\Delta u_{L}^{t,\max}$ are the maximum fluctuation deviation allowed for PV output and load power, respectively, both of which are positive.

The objective of the two-stage robust optimization model for generation load aggregators constructed in this paper is to find the economically optimal scheduling solution for the worst-case scenario of uncertain variables u within an uncertain set $\boldsymbol{U}$, having the following form:

$$\begin{cases} \min\limits_{x}\left\{\max\limits_{u\in U}\ \min\limits_{y\in\Omega(x,u)}\boldsymbol{c}^{T}\boldsymbol{y}\right\} \\ s.t.\quad \boldsymbol{x}=\left(x_{1},x_{2},\cdots,x_{2\times N}\right)^{T} \\ x_{i}\in\{0,1\},\forall i\in(1,2,\cdots 2\times N), \end{cases} \tag{31}$$

where the outer layer is minimized to the first stage master problem with the optimization variable $\boldsymbol{x}$ and the maximum minimization of the inner layer is the second stage subproblem with optimization variables $\boldsymbol{u}$ and $\boldsymbol{y}$. The second stage minimization problem is equivalent to the objective function of Eq. 26, which represents the minimum operating cost. The expressions for $\boldsymbol{x}$ and $\boldsymbol{y}$ are shown in Eq. 28. $\Omega(\boldsymbol{x},\boldsymbol{u})$ denotes the feasible domain of the optimization variables $(\boldsymbol{x},\boldsymbol{u})$ given a set of $\boldsymbol{y}$. The specific expressions are as follows:

$$\Omega(\boldsymbol{x},\boldsymbol{y})=\begin{Bmatrix} \boldsymbol{y}\,| & \\ \boldsymbol{A}\boldsymbol{y}\geq\boldsymbol{d} & \rightarrow\gamma \\ \boldsymbol{K}\boldsymbol{y}=\boldsymbol{0} & \rightarrow\lambda \\ \boldsymbol{G}\boldsymbol{x}+\boldsymbol{E}\boldsymbol{y}\geq\boldsymbol{h} & \rightarrow\nu \\ \boldsymbol{I}_{u}\boldsymbol{y}=\widehat{\boldsymbol{u}} & \rightarrow\pi \end{Bmatrix}, \tag{32}$$

where γ,λ,ν,π denote the pairwise variables corresponding to each constraint in the minimization problem of the second stage.

For each set of uncertain variables $\boldsymbol{u}$, a deterministic optimization model shown by Eq. 26 can be obtained, and the purpose of the max-structure in the robust optimization model is to find the worst-case scenario.

2.3 Column constraint generation algorithm

For the aforementioned two-stage robust optimization model of the generation load aggregator, the column constraint generation algorithm (C and CG) is chosen to solve the model (Fanzeres et al., 2020). The C and CG algorithm is similar to the Benders decomposition algorithm in that the problem is first decomposed into a master problem and a subproblem and solved alternatively to obtain the optimal solution to the original problem (Alvarez et al., 2020). The difference between the two algorithms is that the C and CG algorithm continuously introduces variables and constraints related to the subproblems in the process of solving the master problem to obtain more compact lower bounds on the objective function values, thus reducing the number of iterations (Shi et al., 2020).

The decomposition of Equation 31 yields a master problem of the form

$$\begin{cases} \min\limits_{x}\ \beta \\ s.t.\ \beta\geq\boldsymbol{c}^{T}\boldsymbol{y}_{l} \\ \boldsymbol{A}\boldsymbol{y}_{l}\geq\boldsymbol{d} \\ \boldsymbol{K}\boldsymbol{y}_{l}=\boldsymbol{0} \\ \boldsymbol{G}\boldsymbol{x}+\boldsymbol{E}\boldsymbol{y}_{l}\geq\boldsymbol{h} \\ \boldsymbol{I}_{u}\boldsymbol{y}_{l}=\boldsymbol{u}_{l}^{\star} \\ \forall l\leq k, \end{cases} \tag{33}$$

where k is the current number of iterations; y_l is the solution of the subproblem after the lth iteration; and $\boldsymbol{u}_{l}^{\star}$ is the value of the uncertain variable $\boldsymbol{u}$ under the worst-case scenario obtained after the lth iteration.

The decomposed subproblem takes the form

$$\max_{u\in U}\ \min_{y\in\Omega(x,u)}\boldsymbol{c}^{T}\boldsymbol{y}. \tag{34}$$

From the aforementioned analysis, the inner minimization of Eq. 34 is a linear problem for a given set of $(\boldsymbol{x},\boldsymbol{y})$. According to the strong dual theory and the correspondence of Eq. 32, the problem can be transformed into the max problem and combined with the outer max problem to obtain the dual problem as shown in the following equation:

$$\begin{cases} \max\limits_{u\in U,\gamma,\lambda,\nu,\pi}\boldsymbol{d}^{T}\gamma+(\boldsymbol{h}-\boldsymbol{G}\boldsymbol{x})^{T}\nu+\boldsymbol{u}^{T}\pi \\ s.t.\boldsymbol{A}^{T}\gamma+\boldsymbol{K}^{T}\lambda+\boldsymbol{E}^{T}\nu+\boldsymbol{I}_{u}^{T}\pi\leq c \\ \gamma\geq 0,\nu\geq 0,I_{u}\geq 0, \end{cases} \tag{35}$$

where there exists a bilinear term $\boldsymbol{u}^{T}\pi$. According to the conclusions of the literature (Bertsimas et al., 2013), $\boldsymbol{u}^{\star}$ corresponding to the optimal solution of this pairwise problem is a pole of the uncertainty set $\boldsymbol{U}$; that is, Eq. 35 takes its maximum value when uncertain variable u should be taken to be the boundary of the fluctuation interval described by Eq. 30. In the generation load aggregator, the operating cost of the generation load aggregator is the largest when the PV output is the minimum value and the load power is maximum, which is more consistent with the definition of the "worst-case" scenario. Therefore, Eq. 30 is rewritten in the following form:

$$\boldsymbol{U}=\begin{cases} \boldsymbol{u}=\left[u_{PV}^{t},u_{L}^{t}\right]^{T}\in\mathbb{R}^{(N)\times 2},t=1,2\cdots N_{T} \\ u_{PV}^{t}=\widehat{u}_{PV}^{t}-B_{PV}^{t}\Delta u_{PV}^{t,\max} \\ \sum\limits_{t=1}^{N}B_{PV}^{t}\leq\Gamma_{PV} \\ u_{L}^{t}\in\left[\widehat{u}_{L}^{t}-\Delta u_{L}^{t,\max},\widehat{u}_{L}^{t}+\Delta u_{L}^{t,\max}\right] \\ \sum\limits_{t=1}^{N}B_{L}^{t}\leq\Gamma_{L}, \end{cases} \tag{36}$$

where $\boldsymbol{B}=[B_{PV}^{t},B_{L}^{t}]^{T}$ is a binary variable, and a value of 1 indicates that the uncertain variable is the boundary of the interval at the ecoupled into main time t. Γ_{PV} and Γ_{L} are the "uncertainty regulation parameters" for PV and load, respectively (Wang et al., 2016), which are integers in the range of 0–N and represent the total number of periods in which PV and load take the boundary values of the fluctuation interval in a scheduling cycle. After substituting the expression for the uncertain variables in Eq. 36 into Eq. 35, it will appear in the form of a product of binary and continuous variables, which is linearized by introducing auxiliary

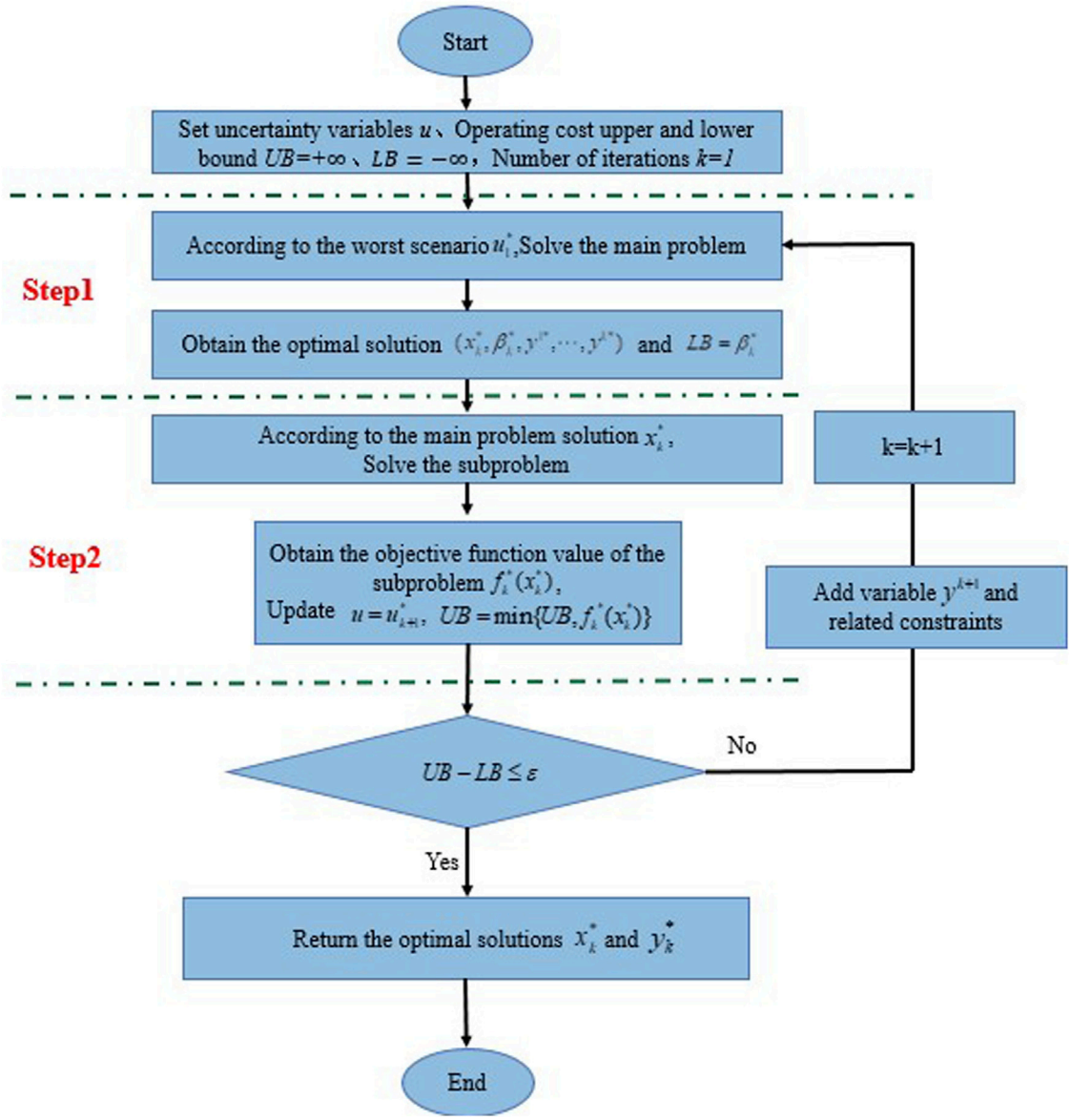

FIGURE 3
Flow chart of the two-stage robust optimization model.

variables and associated constraints (Pistikopoulos, 1998) to obtain the following equation:

$$\begin{cases} \max\limits_{u\in U,\gamma,\lambda,\nu,\pi} \boldsymbol{d}^T\gamma + (\boldsymbol{h} - \boldsymbol{G}\boldsymbol{x})^T\nu + \widehat{\boldsymbol{u}}^T\pi + \Delta\boldsymbol{u}^T\boldsymbol{B}' \\ s.t. \quad \boldsymbol{A}^T\gamma + \boldsymbol{K}^T\lambda + \boldsymbol{E}^T\nu + \boldsymbol{I}_u^T\boldsymbol{\pi} \le c \\ 0 \le \boldsymbol{B}' \le \bar{\pi}\boldsymbol{B} \\ \pi - \bar{\pi}(1 - \boldsymbol{B}) \le \boldsymbol{B}' \le \pi \\ \sum\limits_{t=1}^{N} B_{PV}^t \le \Gamma_{PV} \\ \sum\limits_{t=1}^{N} B_L^t \le \Gamma_L, \end{cases} \tag{37}$$

where $\Delta\boldsymbol{u} = [\Delta u_{PV}^{t,\max}, \Delta u_L^{t,\max}]^T$ and $\boldsymbol{B}' = [B'^{,t}_{PV}, B'^{,t}_{L}]^T$ are continuous auxiliary variables and $\bar{\pi}$ is the upper bound of the pairwise variables and is a sufficiently large positive real number.

After the aforementioned derivation and transformation, the two-stage robust optimization model for the generation load aggregator is decoupled into the main problem and subproblem with a mixed integer linear form, and the model is solved by the C and CG algorithm, shown in Figure 3.

1) The uncertain variable $\boldsymbol{u}$ is set as the initial worst-case scenario, the lower bound $LB = -\infty$, the upper bound $UB = +\infty$, and the number of iterations $k = 1$.
2) The first stage of a two-stage robust optimization: The master problem in Eq. 33 for the optimal solution $(\boldsymbol{x}_k^*, \boldsymbol{\beta}_k^*, \boldsymbol{y}^{1*}, \cdots, \boldsymbol{y}^{k*})$ is solved according to the worst-case scenario $\boldsymbol{u}_1^*$, with the value of the master problem objective function as the new lower bound $LB = \beta_k^*$.
3) The second stage of a two-stage robust optimization: The solution $\boldsymbol{x}_k^*$ of the master problem is substituted into the

TABLE 1 Operating parameters of generation load aggregators.

Unit		Parameter	Value
Micro-gas turbine		P_G^{max}/kW	1,000
		P_G^{min}/kW	100
		$a/b\,(yuan/kW.h)$	0.72/0
Energy storage		P_s^{max}/kW	1,200
		$E_s^{max}/kW.h$	4,500
		$E_s^{min}/kW.h$	800
		$E_s\,(0)/kW.h$	2,500
		$K_s/\,(yuan/kW.h)$	0.62
		η	0.95
Transferable load	Start/stop time delay type	$K_{QT}/\,(yuan/kW.h)$	0.55
		$D_{QT}/kW.h$	6,480
	Power size adjustment type	$K_{GL}/\,(yuan/kW.h)$	0.58
		$D_{GL}/kW.h$	2,140
External grid interactive power		P_M^{max}/kW	6,000

subproblem in Eq. 37 to obtain the objective function value $\boldsymbol{f}_k^*(\boldsymbol{x}_k^*)$ of the subproblem and the uncertain variables $\boldsymbol{u} = \boldsymbol{u}_{k+1}^*$ and the upper bound $UB = \min\left\{UB, \boldsymbol{f}_k^*(\boldsymbol{x}_k^*)\right\}$ are updated.

4) The convergence threshold is set to ε. If $UB - LB \le \varepsilon$, the iteration is stopped and the optimal solutions $\boldsymbol{x}_k^*$ and $\boldsymbol{y}_k^*$ are returned. Otherwise, the variable $\boldsymbol{y}^{k+1}$ and the following constraint are added:

$$\begin{cases} \beta \ge \boldsymbol{c}^T \boldsymbol{y}_{k+1} \\ \boldsymbol{A}\boldsymbol{y}_{k+1} \ge \boldsymbol{d} \\ \boldsymbol{K}\boldsymbol{y}_{k+1} = \boldsymbol{0} \\ \boldsymbol{G}\boldsymbol{x} + \boldsymbol{E}\boldsymbol{y}_{k+1} \ge \boldsymbol{h} \\ \boldsymbol{I}_u \boldsymbol{y}_l = \boldsymbol{u}_{k+1}^*. \end{cases} \tag{38}$$

Let $k = k + 1$, and we skip to 2) until the algorithm converges.

3 Results and discussion

The generation load aggregator shown in Figure 1 is used as an example for this study. The simulation analysis includes three aspects: economic scheduling of generation load aggregator, comparison among optimization models, and boundary conditions of energy storage scheduling.

3.1 Economic dispatch scheme for generation load aggregators

In the economic scheduling scheme of the generation load aggregator, the uncertainty regulation parameter of the load power is set to 12, which means that the load power will reach the maximum value of the forecast interval for at most 12 periods during the scheduling optimization process (Liu et al., 2018). The uncertainty regulation parameter of the PV output is set to 6, which means that the minimum value of the forecast interval will be reached for at most six periods during the optimization process and the rest of the periods will be equal to the forecast value. The operating parameters of the generation load aggregator during the simulation are shown in Table 1(Li, 2020).

In practice, the maximum allowed fluctuation deviation of load power and PV output within the generation load aggregator can be set based on the historical forecast deviation in the past. This article takes as an example a typical weekday on a sunny spring day in Yongqiang Industrial Park in Shenyang, Liaoning Province, China. The predicted curves and actual curves of its load power and photovoltaic output are shown in Figures 4A,B, respectively. Also, the shaded parts are the uncertainty sets considered in this paper with values of 10% and 15% of the predicted values of load power and PV output (China, National Education Association, 2013). The residential electricity step tariff of a city in China is used as the day-ahead trading tariff for power exchange between the external grid and the generation load aggregator, as shown in Figure 4C.

The two-stage robust generation load aggregator scheduling optimization process used in this example is shown in Figure 5A, and it stabilized in the 2nd iteration.

The scheduling results are shown in Figures 5A-E. Figure 5B shows the overall results of the two-stage robust generation load aggregator optimized scheduling. Figure 5C shows the micro-gas turbine output power and the power purchased and sold by the generating load aggregator to the external grid, taking negative values when the generating load aggregator purchases power from the external grid. Figure 5D shows the energy storage charging and discharging power, negative when charging and positive when discharging. Figure 5E shows the start–stop time delay transferable load actual and desired power usage schedule. Figure 5F shows the power sizing transferable load actual and desired power usage schedule.

As shown in Figure 5B, in 1–7 h and 19–24 h, the PV output is 0, and the load of the generation load aggregator relies entirely on the micro-gas turbine, energy storage, and external grid supply. At this time, when the day-ahead traded tariff of the external grid is lower than the unit power generation cost of the micro-gas turbine, the micro-gas turbine operates at the minimum output power, as shown in Figure 5C for 1–7 h and 24 h. During the rest of the period, the micro-gas turbine outputs maximum power, reducing the purchased power to the external grid (e.g., 8 h, 12–22 h, and 24 h) and selling power to the external grid during peak tariff hours (e.g., 9–11 h and 23 h), thus reducing operating costs.

As can be seen in Figure 5D, under the time-sharing tariff mechanism and the periodic conditions of PV output, the charging of energy storage units during lower tariff hours or PV output hours, such as 5–6 h, 16–18 h, and 24 h, and discharging during peak tariff hours, such as 9–11 h and 21–23 h, can achieve not only peak shaving and valley filling but also lower operating costs. As shown in Figure 5E, the expected electricity consumption plan for the start–stop time delay type of transferable load is not much different from the peak and valley values of the load compared to the conventional load due to the three shifts. However, the system reformulates the production plan without affecting the conditions of production,

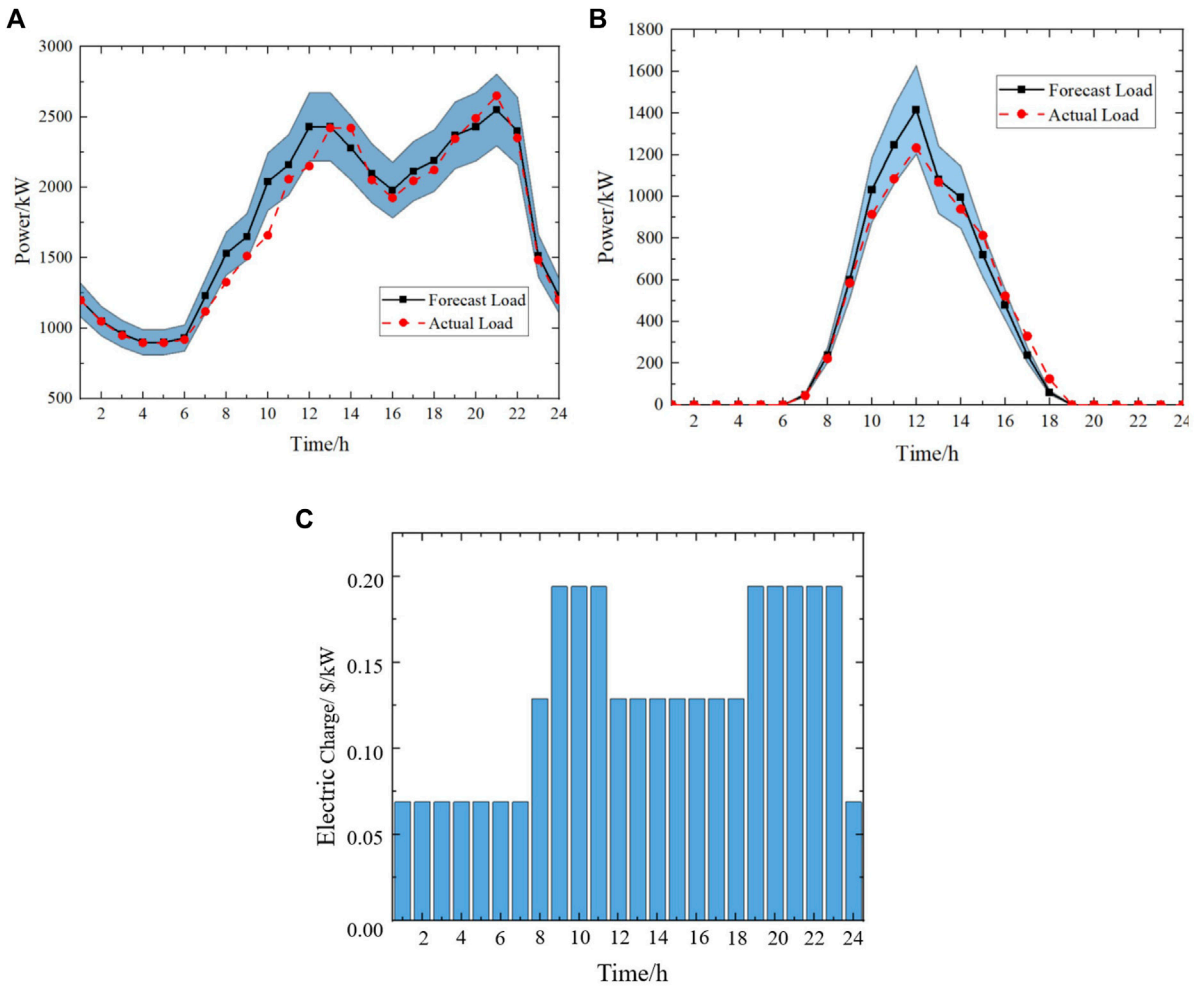

FIGURE 4
(A) Forecast/actual load power curve of a typical working day at Yongqiang Industrial Park in Shenyang, **(B)** forecast/actual PV output curve for a typical working day at Yongqiang Industrial Park in Shenyang, and **(C)** external grid day trading tariff.

advance, or stagger part of the load. The system will arrange as many loads with large power as possible during the period of low electricity prices, such as transferring part of the electricity power from 11–13 h to 6–8 h and transferring part of the electricity power from 18–23 h to 24–5 h. Because the system works 24 h a day, the operational space for load shifting is not very large. This observation was also made by Chen (2020). As shown in Figure 5F, the desired electricity consumption schedule for the power sizing type of transfer loads is similar to that of conventional loads, with electricity consumption mainly concentrated in peak tariff hours. Under the premise of satisfying the total electricity demand and the electricity consumption constraint of each period, the power consumption in the 11–24 h period is reduced and the power consumption in the 1–10 h period is increased, thus reducing the power that the generation load aggregator needs to purchase in the peak tariff period.

3.2 Comparison of the system with and without generation load aggregators

In the absence of a generation load aggregator, small- and medium-sized transferable loads can only be purchased from the external grid as non-regulated loads, without subsidies for peak and valley shifting, because their electricity consumption and regulation do not meet the requirements for participation in the electricity market. Power generation and energy storage cannot participate in power market trading due to the small installed capacity, and the electricity generated will not be sold to the external grid and can only be used as a self-provided generator for the load (Khan et al., 2021; Wu et al., 2022a). Its daily operating cost is shown in Eq. 39, with constraints as in Eq. 2, Eq. 4–Eq. 7, and Eq. 23.

$$\min C' = \sum_{t=1}^{N} [C_G^t + C_S^t + C_L^t + C_M^t], \tag{39}$$

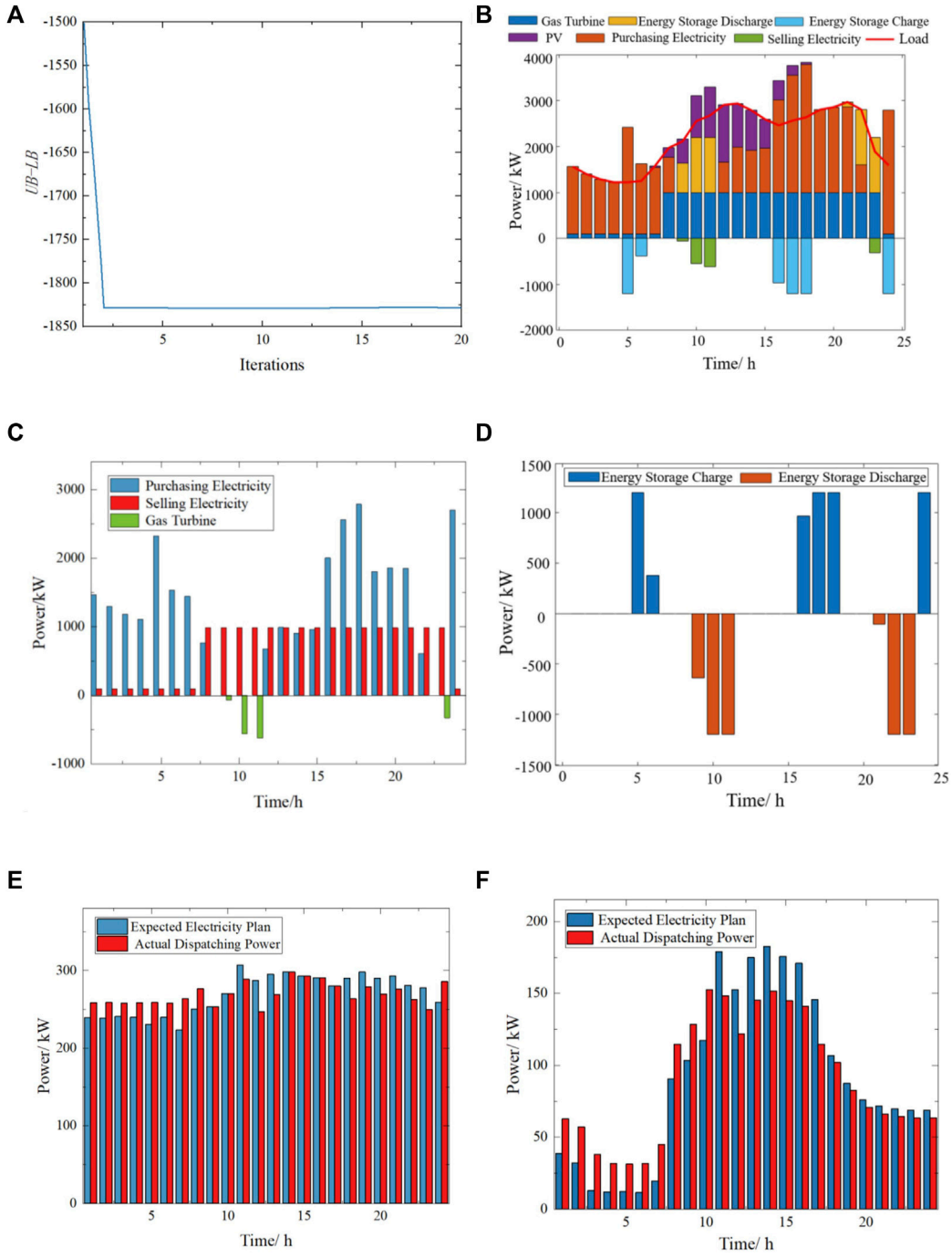

FIGURE 5
(A) Two-stage robust generation load aggregator scheduling optimization process, **(B)** power of each component within the generation load aggregator after two-stage robust optimization, **(C)** micro-gas turbine output power and generation load aggregation commercial power purchase and sale, **(D)** energy storage charging and discharging power, **(E)** start/stop time delay type transferable load actual/desired power consumption plan, and **(F)** power sizing-type transferable load actual/desired electricity usage plan.

TABLE 2 Comparison of operating costs of systems optimized with and without generation load aggregators.

	With generation load aggregator	Without generation load aggregator
Day-ahead operating cost/$	5,124	5,249

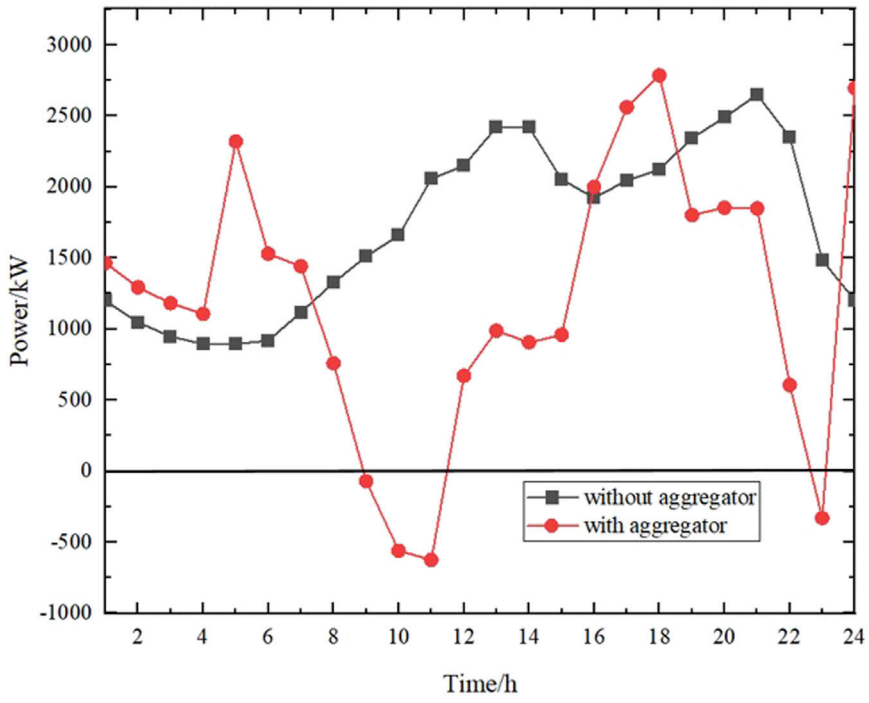

FIGURE 6
Comparison of power purchased from the grid by loads with and without generation load aggregator.

where C_L^t is the cost of electricity for the load. The operating costs of the optimized system with and without generation load aggregators are shown in Table 2, which shows that the operating costs of the system with generation load aggregators are significantly lower than those without generation load aggregators because generation load aggregators sell electricity when prices are high and buy it when prices are low through price differentials. The comparison of load purchases from the grid in the case of generation load aggregators and the traditional dispatch mode is shown in Figure 6. If no generation load aggregator exists, although each load has its own distributed PV, which can reduce the load during the noon hour, the electricity consumption period of 19–22 h is still a peak. If a generation load aggregator exists, the internal transferable load can participate in the power market through the generation load aggregator to shift the peak and fill the valley in exchange for subsidies and reduce the cost of electricity. The generation and storage facilities can participate in the power market through the generation load aggregator as a power source to supply electricity to the external grid to gain profit. In addition, in the presence of a generation load aggregator, the load gets a certain degree of rise during the trough period of electricity consumption in the external grid, and in some areas where renewable energy is more concentrated, the generation load aggregator can promote the consumption of renewable energy. In contrast, during the peak periods of the external grid, the demand of the generation load aggregator to purchase power from the outside is low, and it can even serve as a temporary power source to supply the external grid. Also, during peak periods on the external grid, as can be seen in the 9–13 time period, although the system's electricity consumption is at its peak, the generating load aggregator has a very low need to purchase power from the outside world and is even able to act as a temporary source of power to the external grid when the price of electricity is high. Generation load aggregators have a peak shifting effect, shifting the high point of the evening peak of the required purchased power from the 20–22 time period to the 16–17 time period. Electricity prices are low during the 6–17 time period because it is not the peak of electricity consumption on the external grid. Reducing the cost of electricity consumption also contributes to mitigating peak-to-valley differences in the external grid. So, power prices are low, reducing the cost of electricity while also contributing to the external grid to mitigate peak-to-valley differences. In summary, generation load aggregators can relieve peak and valley pressure on the external grid from the load side.

Table 3 shows the comparison of the cost of electricity consumption for each type of load with and without generation load aggregators. The costs of electricity consumption for the start/stop time delay-type transferable load, power sizing-type transferable load, and the non-regulated load are $696, $229, and $3,796, respectively, in the absence of a generation load aggregator. With load aggregators, the cost of electricity drops to $563, $84, and $3,786, respectively. Power sizing-type transferable load has the largest percentage reduction in electricity costs due to its deeper involvement in peak shaving and valley filling. The non-regulated load does not participate in peak and valley reduction, but the cost of electricity consumption is reduced due to the presence of generation and storage components. In summary, the rationale for the participation of each type of load in the generation load aggregator and the function of the generation load aggregator to reduce the cost of electricity for the load can be demonstrated.

TABLE 3 Comparison of electricity costs for various types of loads with and without generation load aggregators.

Mode	Cost of electricity consumption/$		
	Start/stop time delay-type transferable load	Power sizing-type transferable load	Non-regulated load
Without generation load aggregator	696	229	3,796
With generation load aggregator	563	84	3,786

TABLE 4 Parameterization of deterministic optimization models in three scenarios.

Scenario	Load power	Photovoltaic power output
1	9–12,16–23h	10–14h,16h
2	7–13h,18–22h	9–14h
3	7–13h,18–22h	10–14h,16h

TABLE 5 Comparison of operation cost between the robust optimization model and deterministic optimization model.

Optimization method	Previous operating cost/$
Robust optimization	5,124
Scenario 1	5,086
Scenario 2	5,034
Scenario 3	5,124

3.3 Comparison of optimization models

The two-stage robust generation load aggregator optimization model proposed in this paper and the deterministic optimization model (Hansen et al., 2015) are compared in two dimensions: the effectiveness of determining the worst-case scenario and the performance of the chosen method.

The two-stage robust generation load aggregator optimization model is based on the uncertainty regulation parameters $\Gamma_L = 12$ and $\Gamma_{PV} = 6$. The worst-case scenario is that the load power takes the maximum value of the prediction interval 12 times from 7 to 13 h and 18–22 h, and the PV output takes the minimum value of the interval six times from 10 to 14 h and 16 h. The deterministic optimization model for the control group is shown in Equation 23 and is solved using a mixed integer linear programming approach. To verify that the scenarios taken from the robust optimization model scheduling scheme selected in the paper are the worst-case scenarios. Several times were randomly selected as the boundary of the prediction interval in the model. It is shown in Table 4 for the following three comparative scenarios.

The two-stage robust generation load aggregator optimization model and three deterministic optimization models were used to solve the day-ahead operating costs of the generation load aggregators, and the results are shown in Table 4. In Scenario 1, the load power is taken to all peak hour tariff periods as the maximum period of the forecast interval. In Scenario 2, the PV output minimum period of the deterministic optimization model increases the peak tariff period by 9 h compared to the robust model. However, the day-ahead operating costs of both scenarios are lower than the results of Scenario 3. The time selected for Scenario 3 is the same as that for the deterministic optimization model, and the day-ahead operating cost is also the same.

To verify the flexibility of the two-stage robust generation load aggregator optimization model to adjust the conservativeness of the scheduling scheme, five sets of uncertainty regulation parameters, as well as a set of deterministic optimization models, are selected to compare the results. The parameter settings, corresponding day-ahead operating costs, purchased power, and sold power are shown in Table 5.

As can be seen from Table 6, the results of the uncertainty robust optimization model are the same as those of the deterministic optimization model with a day-ahead operating cost of $4,575 for the uncertainty adjustment parameter. As the uncertainty in the regulation parameters increases, the operating cost of the generation load aggregator increases as well, amounting to $5,346 for groups $\Gamma_L = 24$ and $\Gamma_{PV} = 12$. In other words, the more the generation load aggregator considers the uncertainty of the load power and PV output when developing the day-ahead dispatch planning scheme, the more conservative the scheme obtained and the higher the operating cost. The change in operating costs is mainly due to the change in power purchased and sold by the generation load aggregator to the external grid. The larger the value of the uncertainty parameter Γ, the greater the number of periods in which the load power is taken to the maximum value of the forecast interval and the PV output is taken to the minimum value of the forecast interval. Therefore, the higher the surplus power of the load aggregator, the higher the total purchased power.

The operating cost of the generation load aggregator using the deterministic optimization model in Table 6 is smaller than that of the robust optimization model, but this does not mean that the deterministic optimization model is “better” than the robust model. The generation load aggregator needs the corresponding generation and consumption plan submitted in the day-ahead market, and the inequality between the planned generation and the actual volume on day 2 caused by the forecast error needs to be purchased in the real-time market (Lankeshwara et al., 2022). Electricity purchase prices in the real-time market are generally higher than those in the day-ahead market, and electricity sales prices are generally lower than those in the day-ahead market (Agrawal, 2022), so forecast errors can lead to higher final transaction costs. In summary, the scheduling

TABLE 6 Day-ahead operating costs and purchased/sold power for generation load aggregators with different uncertainty regulation parameters.

Uncertainty parameter	Previous operating cost/$	Purchased power/kWh	Sold power/kWh
Deterministic optimization	4,575	27,958	1,392
$\Gamma_L = 0, \Gamma_{PV} = 0$	4,575	27,958	1,392
$\Gamma_L = 6, \Gamma_{PV} = 3$	4,903	28,489	1,368
$\Gamma_L = 12, \Gamma_{PV} = 6$	5,124	28,983	1,174
$\Gamma_L = 18, \Gamma_{PV} = 9$	5,178	29,432	1,082
$\Gamma_L = 24, \Gamma_{PV} = 12$	5,346	30,803	908.2

TABLE 7 Comparison of the final operating costs of the system after optimization by robust and deterministic optimization methods.

Robust optimization			Deterministic optimization		
Day-ahead operating cost/$	Equilibrium cost/$/$	Total cost/$	Day-ahead operating cost/$	Equilibrium cost/$	Total cost/$
5,124	287	5,411	4,575	1,285	5,860

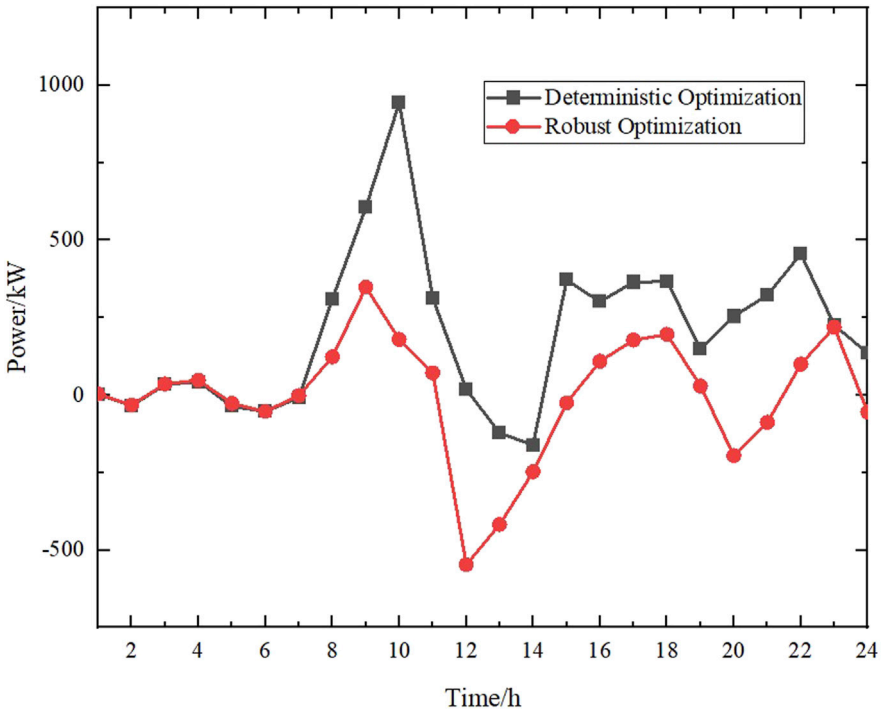

FIGURE 7
Imbalance power generated by real-time power markets.

scheme obtained from the robust optimization model has stronger robustness and the ability to resist the risk of real-time market price fluctuations. To verify the aforementioned conclusions, the performance of the two-stage robust optimization method and the deterministic optimization method proposed in this paper is compared with $\Gamma_L = 12$ and $\Gamma_{PV} = 6$ as examples. The electricity purchase price in the real-time market is assumed to be 1.5 times the price of the corresponding period in the previous day's market, and the electricity sale price is assumed to be 0.5 times the price of the previous day's market. The final operating costs for the robust optimization method and the deterministic optimization method are shown in Table 7, using the actual and predicted values of load and PV shown in Figures 5A,B as references. The balancing operating comparison is shown in Figure 7, with positive values indicating the additional power that the generation load aggregator needs to purchase in the real-time market and negative values indicating the additional power sold by the

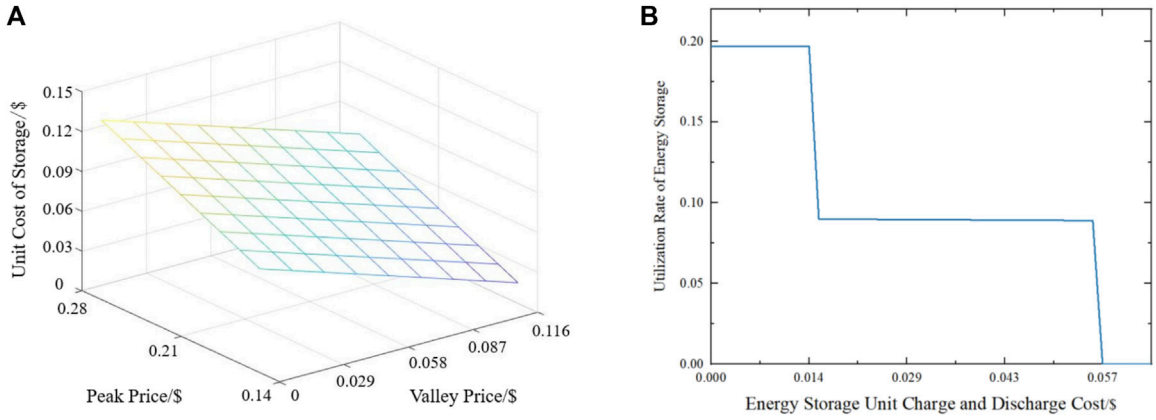

FIGURE 8
(A) Generation load aggregator scheduling energy storage boundary conditions and **(B)** energy storage utilization.

generation load aggregator. The power purchased in the real-time market by the day-ahead scheduling scheme using robust optimization is much less than that of the deterministic optimization method. This results in an equilibrium cost of $287, which is much lower than the equilibrium cost of $5,411 for the deterministic optimization method, thus reducing the final operating cost from $5,860 to $5,411.

3.4 Energy storage scheduling boundary conditions

The time-sharing tariff mechanism between the generation load aggregator and the external grid shown in Figure 7 allows the generation load aggregator to use energy storage to utilize the power purchased in the valley hours in the peak hours under the condition that the energy storage portion of the generation load aggregator needs to meet the constraint (Agrawal, 2022). Based on this premise, the boundary conditions for the use of energy storage for peak shaving by generation load aggregators can be further deduced; in other words, generation load aggregators will use energy storage only under the condition that energy storage can reduce the operating cost of the system. The dispatch cost of energy storage is less than or equal to the difference between the revenue from power sales during peak hours and the cost of power purchases during valley hours (Yang et al., 2020).

$$\left[\eta\sum_{t=1}^{N}P_S^{t,ch}\Delta t+\frac{1}{\eta}\sum_{t=1}^{N}P_S^{t,dis}\Delta t\right]K_S\le\sigma_2\sum_{t=1}^{N}P_S^{t,dis}\Delta t-\sigma_1\sum_{t=1}^{N}P_S^{t,ch}\Delta t, \quad (40)$$

where σ_1 and σ_2 are the traded tariffs for the valley and peak hours, respectively. According to Eq. 6, Eq. 41 can be further simplified as

$$K_S\le\frac{\eta\sigma_2-\sigma_1/\eta}{2}. \quad (41)$$

Equation 41 is the boundary condition for the use of energy storage for peak and valley reduction by generation load aggregators, and its value depends on the relationship between the unit charge and discharge cost of energy storage and the peak and valley tariffs (Talluri et al., 2021). Using the parameters in Table 1 as an example, the generation load aggregator dispatches energy storage boundary conditions as shown in Figure 8A. When the value of K_S is below the plane shown in Figure 16, the generation load aggregator schedules energy storage to reduce the total operating cost; conversely, the generation load aggregator will not schedule the charging and discharging of energy storage.

In the time-sharing tariff mechanism shown in Figure 6, the peak hour tariff is $0.194/(kW·h) and the valley hour tariff is $0.069/(kW·h), and the boundary condition for energy storage dispatched by the generation load aggregator can be obtained from Eq. 41 as K_S is not greater than $0.057/(kW·h). To verify the validity of the aforementioned conclusions, the ratio of the total amount of electricity charged or discharged by the generation load aggregator to the rated capacity of the energy storage during a dispatch cycle is defined as *lth* (Karimi and Kwon, 2021).

$$\theta=\left[\eta\sum_{t=1}^{N}P_S^{t,ch}\Delta t\right]\Big/C_S, \quad (42)$$

where C_S is the rated capacity of the energy storage. As K_S varies, the variation curve of energy storage usage by generation load aggregators is shown in Figure 8A.

As can be seen in Figure 8B, when the unit charge/discharge cost of energy storage is greater than $0.057/(kW·h), the generation load aggregator will no longer charge/discharge energy storage. In other words, in practical application, if the unit charging and discharging cost of energy storage is higher than the boundary condition of energy storage dispatch under the corresponding time-sharing tariff mechanism, energy storage can be installed without other incentive mechanisms.

4 Conclusion

In this paper, the concept of generation load aggregator is proposed to address the problem that small- and medium-sized regulating customers have fewer ways to participate in the electricity market. A

generation load aggregator framework is established that can internally include self-provided generator, energy storage, renewable distributed power, two types of transferable loads, and non-regulated loads. Considering the uncertainty of renewable power sources and loads within the generation load aggregator, this paper establishes a two-stage robust generation load aggregator model to optimize its economic dispatch. To relieve the pressure on the power system from the load side during special hours such as peak and valley and to provide a theoretical basis for future investment and construction planning by generation load aggregator investors and for small- and medium-sized adjustable users to enter the electricity market, the results are analyzed as follows:

(1) The proposed model of generation load aggregator considering uncertainty can be solved by column constraint generation algorithm to obtain the most economical scheduling scheme under the "worst-case" scenario. In this scheme, the generation load aggregator can make full use of self-provided generator, energy storage, and transferable load to reduce the power cost of the system.
(2) A comparison of the results with and without generation load aggregators illustrates the rationality of the generation load aggregator framework by relieving peak and valley pressure on the external grid from the load side, reducing the cost of electricity for loads, and promoting the consumption of renewable energy.
(3) The optimization method used in this paper reduces the operating cost from \$5,860 to \$5,411 compared to the deterministic optimization method, and the resulting day-ahead scheduling scheme is more robust and resilient to the risk of real-time market price fluctuations. Also, the optimization algorithm used in this paper can adjust the conservativeness of the generation load aggregator optimization scheme by varying the uncertainty regulation parameters to accommodate the use of generation load aggregator operators with different mental risk-taking capabilities. The power generation load aggregators with weak psychological risk-taking ability choose the scheme with high conservative type and the uncertainty regulation parameters are larger.
(4) The scheduling plan for energy storage by the generation load aggregator depends on the relationship between the peak tariff, the valley tariff, and the unit charge/discharge cost of energy storage under the time-sharing tariff mechanism. By analyzing the utilization rate curve of energy storage, the energy storage will no longer be meaningful for generation load aggregators when the unit charge/discharge cost of energy storage is greater than \$0.057/(kW·h) under the existing tariff conditions. The findings can provide a reference for generation load aggregator investors when planning whether to install energy storage or the scale of energy storage installation and also help the power market management to design reasonable incentive mechanisms.

Data availability statement

The original contributions presented in the study are included in the article/supplementary material; further inquiries can be directed to the corresponding author.

Author contributions

HZ: conceptualization, data curation, formal analysis, funding acquisition, investigation, methodology, project administration, resources, software, validation, visualization, writing–original draft, and writing–review and editing. YT: conceptualization, funding acquisition, resources, supervision, validation, and writing–review and editing. YZ: conceptualization, methodology, project administration, and writing–review and editing. QL: formal analysis, validation, visualization, and writing–review and editing. NZ: funding acquisition and writing–review and editing.

Funding

The authors declare that financial support was received for the research, authorship, and/or publication of this article. This study was supported by a grant from the National Natural Science Foundation of China-Liaoning Joint Fund (No. 61903264).

Conflict of interest

The authors declare that the research was conducted in the absence of any commercial or financial relationships that could be construed as a potential conflict of interest.

Publisher's note

References

Agrawal, A. (2022). Real Time Market (RTM) at Indian power exchanges: need, short term assessment and opportunities. *Energy Policy* 162, 112810. doi:10.1016/j.enpol.2022.112810

Alvarez, E. F., Paredes, M., and Rider, M. J. (2020). Semidefinite relaxation and generalised benders decomposition to solve the transmission expansion network and reactive power planning. *IET Generation, Transm. Distribution* 14, 2160–2168. doi:10.1049/iet-gtd.2019.0331

Alvim, A. C., Ferreira, J. R., and Pereira, R. B. D. (2021). The enhanced normalized normal constraint approach to multi-objective robust optimization in helical milling process of AISI H13 hardened with crossed array. *Int. J. Adv. Manuf. Technol.* 119, 2763–2784. doi:10.1007/s00170-021-08259-w

Bertsimas, D., Litvinov, E., Sun, X. A., Zhao, J., and Zheng, T. (2013). Adaptive robust optimization for the security constrained unit commitment problem. *IEEE Trans. Power Syst.* 28, 52–63. doi:10.1109/tpwrs.2012.2205021

China, National Education Association (2013). *Technical requirement of power forecasting system for PV power station*.

Chen, X., Xu, X., Dai, X., Hu, Q., Quan, X., and Yang, S. (2021). Strategic interaction to reduce customer fatigue in load aggregation. *Energy Rep.* 7, 339–348. doi:10.1016/j.egyr.2021.08.039

Chen, Y. (2020). *Research on trading mechanism of demand side response in the electricity market*.

Fanzeres, B., Street, A., and Pozo, D. (2020). A column-and-constraint generation algorithm to find nash equilibrium in pool-based electricity markets. *Electr. Power Syst. Res.* 189, 106806. doi:10.1016/j.epsr.2020.106806

Hansen, T. M., Roche, R., Suryanarayanan, S., Maciejewski, A. A., and Siegel, H. J. (2015). Heuristic optimization for an aggregator-based resource allocation in the smart grid. *IEEE Trans. Smart Grid* 6, 1785–1794. doi:10.1109/tsg.2015.2399359

Iria, J., Scott, P., and Attarha, A. (2020). Network-constrained bidding optimization strategy for aggregators of prosumers. *Energy* 207, 118266. doi:10.1016/j.energy.2020.118266

Jiang, M., Wang, X., Dai, F., Xu, L., Wen, X., and Shen, R. (2021). Operation control strategy of load aggregator based on new energy consumption in power grid. *J. Phys. Conf. Ser.* 1894 (6pp), 012026. doi:10.1088/1742-6596/1894/1/012026

Karimi, S., and Kwon, S. (2021). Comparative analysis of the impact of energy-aware scheduling, renewable energy generation, and battery energy storage on production scheduling. *Int. J. Energy Res.* 45, 18981–18998. doi:10.1002/er.6999

Khan, S. U., Mehmood, K. K., Haider, Z. M., Rafique, M. K., Khan, M. O., and Kim, C.-H. (2021). Coordination of multiple electric vehicle aggregators for peak shaving and valley filling in distribution feeders. *Energies* 14, 352. doi:10.3390/en14020352

Kim, D., Cheon, H., Choi, D. G., and Im, S. (2022). Operations research helps the optimal bidding of virtual power plants. *Inf. J. Appl. Anal.* 52, 344–362. doi:10.1287/inte.2022.1120

Kim, H. J., Kim, M. K., and Lee, J. W. (2021). A two-stage stochastic p-robust optimal energy trading management in microgrid operation considering uncertainty with hybrid demand response. *Int. J. Electr. Power and Energy Syst.* 124, 106422. doi:10.1016/j.ijepes.2020.106422

Kumar, T., Kumar, N., Thakur, T., and Nema, S. (2022). Charge scheduling framework with multiaggregator collaboration for direct charging and battery swapping station in a coupled distribution-transportation network. *Int. J. Energy Res.* 46, 11139–11162. doi:10.1002/er.7915

Lankeshwara, G., Sharma, R., Yan, R., and Saha, T. K. (2022). A hierarchical control scheme for residential air-conditioning loads to provide real-time market services under uncertainties. *Energy* 250, 123796. doi:10.1016/j.energy.2022.123796

Li, J. (2020). *Research on the optimization model of purchase and sale of electricity retailers considering demand response*.

Li, S., Zhang, L., Nie, L., and Wang, J. (2022). Trading strategy and benefit optimization of load aggregators in integrated energy systems considering integrated demand response: a hierarchical stackelberg game. *Energy* 249, 123678. doi:10.1016/j.energy.2022.123678

Li, X., and Wang, D. (2021). Does transfer payments promote low-carbon development of resource-exhausted cities in China? *Earth's Future* 10. doi:10.1029/2021ef002339

Liu, Y., Guo, L., and Wang, C. (2018). Two-stage robust optimal economic dispatching method for microgrid. *Proc. CSEE* 14, 4013–4022. doi:10.13334/j.0258-8013.pcsee.170500

Lu, X., Xia, S., Gu, W., Chan, K. W., and Shahidehpour, M. (2021). Two-stage robust distribution system operation by coordinating electric vehicle aggregator charging and load curtailments. *Energy* 226, 120345. doi:10.1016/j.energy.2021.120345

Najafi, A., Pourakbari-Kasmaei, M., Jasinski, M., Lehtonen, M., and Leonowicz, Z. (2021). A hybrid decentralized stochastic-robust model for optimal coordination of electric vehicle aggregator and energy hub entities. *Appl. Energy* 304, 117708. doi:10.1016/j.apenergy.2021.117708

Nguyen, D. T., and Le, L. B. (2015). Risk-constrained profit maximization for microgrid aggregators with demand response. *IEEE Trans. Smart Grid* 6, 135–146. doi:10.1109/tsg.2014.2346024

Pistikopoulos, E. N. (1998). C.A. Floudas, nonlinear and mixed-integer optimization. Fundamentals and applications. *J. Glob. Optim.* 12, 108–110.

Sambodo, M. T., Yuliana, C. I., Hidayat, S., Novandra, R., Handoyo, F. W., Farandy, A. R., et al. (2022). Breaking barriers to low-carbon development in Indonesia: deployment of renewable energy. *Heliyon* 8, e09304. doi:10.1016/j.heliyon.2022.e09304

Sheikhahmadi, P., Mafakheri, R., Bahramara, S., Damavandi, M., and CatalãO, J. (2018). Risk-based two-stage stochastic optimization problem of micro-grid operation with renewables and incentive-based demand response programs. *Energies* 11, 610. doi:10.3390/en11030610

Shi, S., Chen, J., Zhang, Y., and Huang, G. 2020. Optimal operation strategy for micro-energy grid based on the C&CG algorithm. 2020 IEEE 3rd student conference on electrical machines and systems (SCEMS). 04-06 December 2020. Jinan, China. doi:10.1109/SCEMS48876.2020.9352423

Talluri, G., Lozito, G. M., Grasso, F., Iturrino Garcia, C., and Luchetta, A. (2021). Optimal battery energy storage system scheduling within renewable energy communities. *Energies* 14, 8480. doi:10.3390/en14248480

Vahid-Ghavidel, M., Javadi, M. S., Santos, S. F., Gough, M., Mohammadi-Ivatloo, B., Shafie-Khah, M., et al. (2021). Novel hybrid stochastic-robust optimal trading strategy for a demand response aggregator in the wholesale electricity market. *IEEE Trans. Industry Appl.* 57, 5488–5498. doi:10.1109/tia.2021.3098500

Vatandoust, B., Ahmadian, A., Golkar, M. A., Elkamel, A., Almansoori, A., and Ghaljehei, M. (2019). Risk-averse optimal bidding of electric vehicles and energy storage aggregator in day-ahead frequency regulation market. *IEEE Trans. Power Syst.* 34, 2036–2047. doi:10.1109/tpwrs.2018.2888942

Wang, C., Jiao, B., Guo, L., Tian, Z., Niu, J., and Li, S. (2016). Robust scheduling of building energy system under uncertainty. *Appl. Energy* 167, 366–376. doi:10.1016/j.apenergy.2015.09.070

Wang, C., Zhou, Y., Wu, J., Wang, J., Zhang, Y., and Wang, D. (2015a). Robust-index method for household load scheduling considering uncertainties of customer behavior. *IEEE Trans. Smart Grid* 6, 1806–1818. doi:10.1109/tsg.2015.2403411

Wang, Q., and Nie, X. (2022). A stochastic programming model for emergency supply planning considering transportation network mitigation and traffic congestion. *Socio-Economic Plan. Sci.* 79, 101119. doi:10.1016/j.seps.2021.101119

Wang, R., Wang, P., and Xiao, G. (2015b). A robust optimization approach for energy generation scheduling in microgrids. *Energy Convers. Manag.* 106, 597–607. doi:10.1016/j.enconman.2015.09.066

Wu, H., Wang, J., Lu, J., Ding, M., Wang, L., Hu, B., et al. (2022a). Bilevel load-agent-based distributed coordination decision strategy for aggregators. *Energy* 240, 122505. doi:10.1016/j.energy.2021.122505

Wu, H., Wang, L., Peng, D., and Liu, B. (2022b). Input–output efficiency model of urban green-energy development from the perspective of a low-carbon economy. *Clean. Energy* 6, 141–152. doi:10.1093/ce/zkab061

Xu, N., Xu, N., Ling, Y., Liu, Q., Ma, H., Zhou, B., et al. (2020). Electric vehicles charging management based on flexible load aggregation. in *Earth and environmental science*. Editor T. I. C. SERIES

Xu, Y., Xie, L., and Singh, C. (2010). Optimal scheduling and operation of load aggregator with electric energy storage in power markets. North American Power Symposium (NAPS), Boston, MA, USA, 04-06 August 2011.

Yang, H., Hao, Z., Ma, Y., and Dabo, Z. (2020). An inverse proportion technique based scheduling strategy of energy storage system considering electrical load demand difference. *CSEE J. Power Energy Syst.*

Zhang, J., Zhang, P., Wu, H., Qi, X., Yang, S., and Li, Z. (2018). Two-stage load-scheduling model for the incentive-based demand response of industrial users considering load aggregators. *IET Generation, Transm. Distribution* 12, 3518–3526. doi:10.1049/iet-gtd.2018.0089